Electron–hydrogen-atom ionization collisions at intermediate ($5I_0-20I_0$) and high ($\gtrsim 20I_0$) energies

J. N. Das and Samita Seal

Department of Applied Mathematics, University College of Science, 92 Acharya Prafulla Chandra Road, Calcutta 700009, India

(Received 1 August 1991; revised manuscript received 26 October 1992)

Triple-differential cross sections for ionization of hydrogen atoms by electrons have been calculated both for small- as well as large-momentum-transfer cases at intermediate ($5I_0-20I_0$) and high ($\gtrsim 20I_0$) energies (I_0 being the ionization potential) following a method which uses a final-channel three-particle wave function determined by one of the authors. This wave function resulted from an analysis of the three-particle wave equation in momentum space and is correct to the first order in the interaction potentials. Incidentally, it is also the first-order Faddeev wave function. The wave function has been suitably normalized before it is used. The computed results are generally good. The small-momentum-transfer results are in nice agreement with the experimental data except for a certain angular region which includes the recoil peak. The domain over which the present results agree in trend with the experimental measurements is somewhat larger than that for the distorted-wave-Born-approximation calculation. Large-momentum-transfer results are also in qualitative agreement with experiments. There are indications that quantitatively the present results may be better there. Total-ionization cross-section results are also in excellent agreement with experiment above 200-eV energy. These facts together with the simplicity of the calculation establish that the present method has certain advantages over other existing methods. The present calculation may be the starting point for a more elaborate calculation which will take into account more accurately the correlation and higher-order effects in the final-channel three-particle wave function.

PACS number(s): 34.80.Dp

I. INTRODUCTION

Studies, both theoretical and experimental, of the differential cross sections for electron-atom ionization problems, during the past two decades, have revealed many interesting aspects and mechanisms of the ionization of atoms. Results of these studies also indicate inadequacies of the different existing theories in explaining all the details of the ionization problem. References [1–7] and [8–20] deal with the relativistic and the nonrelativistic domains, respectively. Even the simple case of electron–hydrogen-atom ionization collisions proves to be quite difficult to describe correctly with respect to its various aspects.

In the nonrelativistic studies of triple-differential cross sections (TDCS) for electron–hydrogen-atom ionization collisions, there are two different kinematic regions of great interest. One of these is the Ehrhardt asymmetric kinematic region [8] corresponding to very-small-momentum-transfer cases and the other is the region investigated by Weigold and associates [13,14] corresponding to large- and intermediate-momentum-transfer cases at intermediate ($5I_0-20I_0$) and high ($\geq 20I_0$) energies, I_0 being the ionization potential. At present there exist absolute measured value of the TDCS for different small-momentum-transfer cases at 150 and 250 eV energies belonging to the intermediate-energy range. For large-momentum-transfer cases there exist only some relative measurements for different energies such as 100, 113.6, and 250 eV in the intermediate-energy range and for somewhat larger energy of 413.6 eV, and for various scattering and ejection angles, the scattering being coplanar.

Among the existing theories of ionization, distorted-wave impulse approximation [13,14] (DWIA), distorted-wave Born approximation [14,16] (DWBA), coupled pseudostate calculation, and the calculation due to Brauner, Briggs, and Klar [11] are noteworthy. DWIA is computationally simple but the results may not be very accurate, particularly for small-momentum-transfer cases. DWBA and the pseudostate calculations are more involved. The asymmetric small-momentum-transfer cross-section results of these calculations are of comparable accuracy. The calculation of Brauner, Briggs, and Klar, which uses a three-particle wave function that is exact in the far asymptotic region, gives results which agree qualitatively best with the experimental results. Quantitatively, however, the results may be substantially less than the experimental values in some cases, by about 30% or more, particularly in the binary-peak region. It may be noted here that the binary-peak region gives the most significant contribution to the total cross-section result. Except in one case of the DWBA calculation, these methods have not been tested over wide kinematic conditions. The calculation [14] in which DWBA has been applied for a few large-momentum-transfer cases at a high energy (viz., 413.6 eV) gives a good qualitative description of the experimental results. However, concerning the quantitative agreement, the situation is not that clear, particularly in view of the fact that the results presented there for a small-momentum-transfer case do not agree with the results presented later by McCarthy and Zhang

[16]. DWBA is suitable for the investigation of the TDCS over wide kinematic conditions and also of a variety of other results, such as the single- and the double-differential cross sections and the total cross sections. Total cross-section [17] results obtained by this method are generally good at energies above about ten times the ionization potentials. For double-differential cross sections, discrepancies are noted [18], up to 100% in some cases, for helium.

Now, the distorted-wave-Born-approximation [16] T-matrix element for hydrogen,

$$T=\langle \chi_1^{(-)}(\mathbf{p}_1)\chi_2^{(-)}(\mathbf{p}_2)|\, V_f-U_f|\Psi_0\chi_0^{(+)}(\mathbf{k}_0)\rangle \ ,$$

may be viewed as an approximation to the exact result

$$T=\langle \Phi_f^{(-)}|\, V_f-U_f|\Psi_i^{(+)}\rangle \ , \tag{1a}$$

where $\Psi_i^{(+)}$ is approximated by the product $\Psi_0\chi_0^{(+)}(\mathbf{p}_i)$, Ψ_0 being the atomic wave function and $\chi_0^{(+)}$ being the single-particle scattering wave function for an elastic-channel optical potential.

Here, V_f is the interaction between the projectile and the atom and U_f is the potential used to calculate the final-state wave function $\Phi_f^{(-)}$, where

$$\Phi_f^{(-)}=\chi_1^{(-)}(\mathbf{p}_1)\chi_2^{(-)}(\mathbf{p}_2)$$

and χ_1 and χ_2 are the scattering states of the electron-ion subsystems (i.e., Coulomb waves).

An alternative expression for T is

$$T=\langle \Psi_f^{(-)}|\, V_i|\Phi_i\rangle \ , \tag{1b}$$

where V_i is the interaction in the initial channel, Φ_i is the unperturbed initial-channel wave function, and $\Psi_f^{(-)}$ is the exact final-channel three-particle continuum wave function. Depending on (1b), an approximate calculation method may be obtained by approximating $\Psi_f^{(-)}$ in some way. The calculations of Brauner, Briggs, and Klar [11] and the present calculation follow this line. The wave function used by Brauner, Briggs, and Klar is correct in the far asymptotic region The cross-section results indicate that the wave function may not be that good in the near region.

The wave function we use here is exact to the first order in the interaction potentials and is generally good except in the far asymptotic region, as indicated from the cross-section results presented in Sec. III. The calculation may be improved further, say, by including in the calculation the term F_{40} of Das [21]. The ultimate goal, however, will be to approach the exact wave function $\Psi_f^{(-)}$.

II. THEORY AND CALCULATION

The present theory, as indicated above, uses a first-order three-particle wave function for the final scattering state. The wave function was obtained by Das [21] from a momentum-space analysis of the corresponding wave equation and is exactly the same as the first-order Faddeev [22] wave function. The wave function, however, is not correct in the far asymptotic region and needs further normalization. The normalized wave function is used in Eq. (1b) to get an approximate expression for the T-matrix element. Scattering amplitudes and cross sections are then obtained. Details are given below.

A. T-matrix element and the approximate wave function

The (direct) T-matrix element for ionization of a hydrogen atom by an incident electron is give by Eq. (1b), where

$$\Phi_i(\mathbf{r}_1,\mathbf{r}_2)=\varphi_{1S}(\mathbf{r}_1)e^{i\mathbf{p}_i\cdot\mathbf{r}_2}/(2\pi)^{3/2} \ , \tag{2a}$$

$$V_i(\mathbf{r}_1,\mathbf{r}_2)=1/r_{12}-1/r_2 \ , \tag{2b}$$

and $\Psi_f^{(-)}$ is the solution of the wave equation

$$\left[-\nabla_1^2/2-\nabla_2^2/2+\frac{1}{r_{12}}-\frac{1}{r_1}-\frac{1}{r_2}-E\right]\Psi_f^{(-)}=0 \ , \tag{3}$$

where $\mathbf{r}_1$ and $\mathbf{r}_2$ are the coordinates of the two electrons, $\mathbf{r}_2$ corresponding to the incident electron. Momenta of the ejected, the scattered, and the incident electrons are $\mathbf{p}_1$, $\mathbf{p}_2$, and $\mathbf{p}_i$ and their energies are E_1, E_2, and E_i, respectively. In our present calculation we use the wave function of Das [21], which is correct to first order in the interaction potentials. This wave function was obtained from a momentum-space analysis of a three-particle wave equation. It is interesting to note that this first-order wave function agrees with the first-order Faddeev [22] wave function. The second-order correct result obtained by Das, viz., F_{40} of Ref. [21], is also obtainable from Faddeev equations, viz. Eq. (39) of Ref. [22] after replacing T_{23}, T_{31}, and T_{12} in the kernel by v_{23}, v_{31}, and v_{12}, respectively, and replacing $\Psi^{(1)},\Psi^{(2)}$, and $\Psi^{(3)}$ by corresponding first-order results. However, their integral equation (39) is basically different from the integral equation (7d) of Das [21]. For the long-range potentials, considered here, these integral equations should be considered as formal integral equations which may give important informations about the scattering-state wave functions but do not possess all the nice properties of a Fredholm integral equation with a square-integrable kernel. The above first-order wave function does not satisfy the normalization condition at infinity. We multiply it by a suitable normalization constant N and take it as an approximation for the final scattering state and denote it by $\Psi_f^{o(-)}$.

Thus in our present case

$$\Psi_f^{(-)}\simeq\Psi_f^{o(-)}=N\Phi_f^{(-)}=N\Phi_{\mathbf{p}_1,\mathbf{p}_2}^{(-)} \ , \tag{4a}$$

where

$$\begin{aligned}\Phi_{\mathbf{p}_1,\mathbf{p}_2}^{(-)}(\mathbf{r}_1,\mathbf{r}_2)&=[\varphi_{\mathbf{p}_1}^{(-)}(\mathbf{r}_1)e^{i\mathbf{p}_2\cdot\mathbf{r}_2}+\varphi_{\mathbf{p}_2}^{(-)}(\mathbf{r}_2)e^{i\mathbf{p}_1\cdot\mathbf{r}_1}\\&\quad+\varphi_{\mathbf{p}}^{(-)}(\mathbf{r})e^{i\mathbf{P}\cdot\mathbf{R}}-2e^{i\mathbf{p}_1\cdot\mathbf{r}_1+i\mathbf{p}_2\cdot\mathbf{r}_2}]/(2\pi)^3\end{aligned} \tag{4b}$$

and where

$\mathbf{r}=(\mathbf{r}_2-\mathbf{r}_1)/2$, $\mathbf{R}=(\mathbf{r}_2+\mathbf{r}_1)/2$,

$\mathbf{p}=(\mathbf{p}_2-\mathbf{p}_1)$, $\mathbf{P}=(\mathbf{p}_2+\mathbf{p}_1)$.

Here, $\varphi_{\mathbf{q}}^{(-)}(\mathbf{r})$ is the Coulomb wave given by

$$\varphi_{\mathbf{q}}^{(-)}(\mathbf{r})=e^{\pi a/2}\Gamma(1+i\alpha)e^{i\mathbf{q}\cdot\mathbf{r}}\,{}_1F_1(-i\alpha,1,-i[qr+\mathbf{q}\cdot\mathbf{r}]) , \tag{5}$$

where $\alpha=1/p_1$ for $\mathbf{q}=\mathbf{p}_1$, $\alpha=1/p_2$ for $\mathbf{q}=\mathbf{p}_2$, and $\alpha=-1/p$ for $\mathbf{q}=\mathbf{p}$. The normalization constant N depends on $\mathbf{p}_1$ and $\mathbf{p}_2$. We will indicate in Sec. II C below how we determine this normalization constant. Now we discuss the accuracy of this wave function.

B. Accuracy of the wave function

It will be interesting to see how accurately the above wave function $\Psi_f^{o(-)}$ satisfies the wave equation (3). For this we substitute the above ansatz in the left-hand side of Eq. (3) and get

$$\begin{aligned}(H-E)\Psi_f^{o(-)}(\mathbf{r}_1,\mathbf{r}_2)&=\left[-\nabla_1^2/2-\nabla_2^2/2+\frac{1}{r_{12}}-\frac{1}{r_1}-\frac{1}{r_2}-E\right]\Psi_f^{o(-)}\\&=N\left[\left[\frac{1}{r_{12}}-\frac{1}{r_2}\right]e^{i\mathbf{p}_2\cdot\mathbf{r}_2}[\varphi_{\mathbf{p}_1}^{(-)}(\mathbf{r}_1)-e^{i\mathbf{p}_1\cdot\mathbf{r}_1}]+\left[\frac{1}{r_{12}}-\frac{1}{r_1}\right]e^{i\mathbf{p}_1\cdot\mathbf{r}_1}[\varphi_{\mathbf{p}_2}^{(-)}(\mathbf{r}_2)-e^{i\mathbf{p}_2\cdot\mathbf{r}_2}]\right.\\&\quad\left.+\left[-\frac{1}{r_1}-\frac{1}{r_2}\right]e^{i\mathbf{P}\cdot\mathbf{R}}[\varphi_{\mathbf{p}}^{(-)}(\mathbf{r})-e^{i\mathbf{p}\cdot\mathbf{r}}]\right]\Big/(2\pi)^3 .\end{aligned} \tag{6}$$

When p_1, p_2, and $p=|\mathbf{p}_2-\mathbf{p}_1|$ all become large, then Coulomb waves in Eq. (6) approach plane waves in any bounded domain of the coordinate space and the right-hand side of Eq. (6) becomes small. [Keeping $\mathbf{r}$ fixed, if we let $p\to\infty$, then $\varphi_{\mathbf{p}}(\mathbf{r})\to e^{i\mathbf{p}\cdot\mathbf{r}}$, while keeping $\mathbf{p}$ fixed, if we let $r\to\infty$, then $\varphi_{\mathbf{p}}^{(-)}(\mathbf{r})\not\to e^{i\mathbf{p}\cdot\mathbf{r}}$.] In the limit, the wave equation is exactly satisfied. However, for any finite p_1, p_2, and p, the wave function (4) may not be valid in the far asymptotic region. But this region is not that important, except in determining the normalization of the wave function. The normalization problem will be considered in Sec. II C. Even when one of the momenta, say, p_2, is large and the other one is small, one has approximately

$$(H-E)\Psi_f^{o(-)}\simeq\left[\frac{1}{r_{12}}-\frac{1}{r_2}\right]e^{i\mathbf{p}_2\cdot\mathbf{r}_2}\times[\varphi_{\mathbf{p}_1}^{(-)}(\mathbf{r}_1)-e^{i\mathbf{p}_1\cdot\mathbf{r}_1}]/(2\pi)^3 . \tag{7}$$

This may be compared with the corresponding result for the final unperturbed state that is used in the Born-approximation calculation:

$$(H-E)[\varphi_{\mathbf{p}_1}^{(-)}(\mathbf{r}_1)e^{i\mathbf{p}_2\cdot\mathbf{r}_2}/(2\pi)^3]=\left[\frac{1}{r_{12}}-\frac{1}{r_2}\right]e^{i\mathbf{p}_2\cdot\mathbf{r}_2}\varphi_{\mathbf{p}_1}^{(-)}(\mathbf{r}_1)/(2\pi)^3 . \tag{8}$$

The right-hand side of Eq. (7), which contains a factor that is the difference of a Coulomb wave and the corresponding plane wave, will, in general, be small compared with that in Eq. (8). So in the asymmetric kinematic conditions of Ehrhardt also, the wave function (4) generally satisfies the wave equation better than that used in the first Born calculation. When $\mathbf{p}_1$ will be very close to $\mathbf{p}_2$, which is not true in any of the cases considered here, the wave equation will not be satisfied accurately and the corresponding computed results may not be good.

We next indicate a method of determining approximately the normalization constant N in Eq. (4) which is used in our present calculation.

C. Normalization of the wave function

The exact wave function $\Psi_f^{(-)}=\Psi_{\mathbf{p}_1,\mathbf{p}_2}^{(-)}$ satisfies the normalization condition

$$\left\langle\Psi_{\mathbf{p}_1,\mathbf{p}_2}^{(-)}\middle|\Psi_{\mathbf{q}_1,\mathbf{q}_2}^{(-)}\right\rangle=\delta(\mathbf{q}_1-\mathbf{p}_1)\delta(\mathbf{q}_2-\mathbf{p}_2) . \tag{9}$$

Since an approximate wave function cannot, in general, satisfy the normalization condition (9) exactly, one can only satisfy it approximately. Thus we determine the normalization constant $N=N(\mathbf{p}_1,\mathbf{p}_2)$ in the approximate wave function $\Psi_f^{o(-)}=\Psi_{\mathbf{p}_1,\mathbf{p}_2}^{o(-)}$, given by (4a), from the requirement

$$\left\langle\Psi_{\mathbf{p}_1,\mathbf{p}_2}^{o(-)}\middle|\Psi_{\mathbf{q}_1,\mathbf{q}_2}^{o(-)}\right\rangle\simeq\delta(\mathbf{q}_1-\mathbf{p}_1)\delta(\mathbf{q}_2-\mathbf{p}_2) . \tag{10}$$

This, on integration over $\mathbf{q}_1$ and $\mathbf{q}_2$, gives

$$\int\left\langle\Psi_{\mathbf{p}_1,\mathbf{p}_2}^{o(-)}\middle|\Psi_{\mathbf{q}_1,\mathbf{q}_2}^{o(-)}\right\rangle d^3q_1d^3q_2\simeq 1 . \tag{11}$$

Then one has

$$|N(\mathbf{p}_1,\mathbf{p}_2)|^{-2}\simeq\int\left\langle\Phi_{\mathbf{p}_1,\mathbf{p}_2}^{(-)}|\Phi_{\mathbf{q}_1,\mathbf{q}_2}^{(-)}\right\rangle d^3q_1d^3q_2 . \tag{12}$$

The right-hand side of this relation involves 16 integrals, of which seven may be evaluated exactly. Five of the remaining integrals contain factors of the form $\int\tilde{\varphi}_{\mathbf{q}_1}^{(-)}(\mathbf{p}_1)d^3q_1$, where $\tilde{\varphi}_{\mathbf{q}_1}^{(-)}(\mathbf{p}_1)$ is the Fourier transform of the Coulomb wave function $\varphi_{\mathbf{q}_1}^{(-)}(\mathbf{r})$. The remaining four integrals are of the form

$$\int\tilde{\varphi}_{\mathbf{q}_1}^{(-)*}(\mathbf{q}_1')\tilde{\varphi}_{\mathbf{p}_1}^{(-)}(\mathbf{p}_2-\mathbf{q}_1')d^3q_1d^3q_1' . \tag{13}$$

Numerical evaluation of these integrals is again

difficult. However, these two types of integrals may be evaluated quite accurately by making use of the observation that the Fourier transform $\tilde{\varphi}_{\mathbf{p}_1}^{(-)}(\mathbf{t})$ satisfies the normalization condition

$$\int \tilde{\varphi}_{\mathbf{p}_1}^{(-)*}(\mathbf{t})\tilde{\varphi}_{\mathbf{q}_1}^{(-)}(\mathbf{t})d^3t=\delta(\mathbf{q}_1-\mathbf{p}_1) . \tag{14}$$

Consequently,

$$\int \tilde{\varphi}_{\mathbf{p}_1}^{(-)*}(\mathbf{t})\tilde{\varphi}_{\mathbf{q}_1}^{(-)}(\mathbf{t})d^3t\, d^3q_1=1 . \tag{15}$$

Since $\tilde{\varphi}_{\mathbf{p}_1}^{(-)}(\mathbf{t})$ is highly peaked, approximately as a δ function, at $\mathbf{t}=\mathbf{p}_1$, one can approximate (15) by

$$\left[\int \tilde{\varphi}_{\mathbf{p}_1}^{(-)*}(\mathbf{t})d^3t\right]\left[\int \tilde{\varphi}_{\mathbf{q}_1}^{(-)}(\mathbf{p}_1)d^3q_1\right]\simeq 1 . \tag{16}$$

Now,

$$\int \tilde{\varphi}_{\mathbf{p}_1}^{(-)*}(\mathbf{t})d^3t=\varphi_{\mathbf{p}_1}^{(-)}(o)=e^{\pi\alpha_1/2}\Gamma(1-i\alpha_1) ,$$

where $\alpha_1=1/p_1$ and so

$$\int \tilde{\varphi}_{\mathbf{q}_1}^{(-)}(\mathbf{p}_1)d^3q_1\simeq 1/\varphi_{\mathbf{p}_1}^{(-)*}(o) . \tag{17}$$

Similar techniques may be used to evaluate integrals of the type (13). The final result for the normalization constant is then

$$|N(\bar{\mathbf{p}}_1,\bar{\mathbf{p}}_2)|^{-2}=7-2[\lambda_1+\lambda_2+\lambda_3]-[2/\lambda_1+2/\lambda_2+2/\lambda_3]+[\lambda_1/\lambda_2+\lambda_1/\lambda_3+\lambda_2/\lambda_3+\lambda_2/\lambda_1+\lambda_3/\lambda_1+\lambda_3/\lambda_2]=Me^{i\epsilon}, \tag{18}$$

say, where

$$\lambda_1=e^{\pi\alpha_1/2}\Gamma(1-i\alpha_1),\quad \alpha_1=1/p_1$$
$$\lambda_2=e^{\pi\alpha_2/2}\Gamma(1-i\alpha_2),\quad \alpha_2=1/p_2$$
$$\lambda_3=e^{\pi\alpha/2}\Gamma(1-i\alpha),\quad \alpha=-1/p .$$

Since the relation (10) is not exact, a contribution to the integral (11) also arises from nonneighboring elements. Consequently, one has a nonzero phase factor with the right-hand side of Eq. (18). Numerical results in all cases show that this phase ϵ is small and may be neglected. The smallness of the value of ϵ also partly justifies the approximations used. The absolute value of the right-hand side of Eq. (18) is then taken as an estimate of $|N(\mathbf{p}_1,\mathbf{p}_2)|^{-2}$.

D. Calculation of the *T*-matrix element

The approximate T-matrix element in our present case is

$$T_{fi}=\langle \Psi_f^{o(-)}|V_i|\Phi_i\rangle$$
$$=N(\mathbf{p}_1,\mathbf{p}_2)\langle \Phi_f^{(-)}|V_i|\Phi_i\rangle . \tag{19}$$

Except for two, all integrals in this expression may be evaluated exactly. These two remaining integrals can be reduced to one-dimensional integrals. For this we use the integral representation of the confluent hypergeometric function,

$${}_1F_1(a,c,z)$$
$$=\frac{\Gamma(c)}{\Gamma(a)\Gamma(c-a)}\int_0^1 dx\, x^{a-1}(1-x)^{c-a-1}e^{xz} , \tag{20}$$

in the expression for the Coulomb wave function,

$$\varphi_{\mathbf{p}}^{(-)*}(\mathbf{r})=e^{\pi\alpha/2}\Gamma(1-i\alpha)e^{-i\mathbf{p}\cdot\mathbf{r}}\,{}_1F_1(i\alpha,1,i(pr+\mathbf{p}\cdot\mathbf{r})) . \tag{21}$$

Making use of Lewis's [23] integral result, one can reduce the above two integrals to the form

$$J=C\int_0^1 dx\, x^{i\alpha-1}(1-x)^{-i\alpha}\Psi(x) . \tag{22}$$

For numerical computations it will be convenient to rewrite it as

$$J=C\int_0^1 dx\, x^{i\alpha}(1-x)^{-i\alpha}[\Psi(x)-\Psi(o)]/x$$
$$+C\Gamma(i\alpha)\Gamma(1-i\alpha)\Psi(o) . \tag{23}$$

Such integrals have been numerically evaluated using the Gauss quadrature formula. For the present computation a 40-point formula proved to be sufficient.

The direct scattering amplitude $f(\mathbf{p}_1,\mathbf{p}_2)$ is then determined from

$$f(p_1,p_2)=-(2\pi)^2T_{fi} , \tag{24a}$$

and the exchange amplitude $g(\mathbf{p}_1,\mathbf{p}_2)$ is approximated by

$$g(\mathbf{p}_1,\mathbf{p}_2)=f(\mathbf{p}_2,\mathbf{p}_1) . \tag{24b}$$

The triple-differential cross section is finally given by

$$\frac{d\sigma}{d\Omega_1 d\Omega_2 dE_1}=\frac{p_1p_2}{p_i}[\tfrac{3}{4}|f-g|^2+\tfrac{1}{4}|f+g|^2] . \tag{25}$$

III. RESULTS

Figures 1 and 2 display certain small-momentum-transfer coplanar-scattering cross-section results for the incident-electron energy $E_i=250$ and 150 eV, respectively. Figure 1 displays three sets of results corresponding to (a) $E_1=5$ eV, $\theta_2=3°$; (b) $E_1=5$ eV, $\theta_2=8°$, and (c) $E_1=14$ eV, $\theta_2=8°$. These results are compared with the DWBA results and with the results of Brauner, Briggs, and Klar [11] only. The experimental results we compare with are the relative measurements of Lohmann *et al.* [24] normalized to a point of the second Born results in each case and the absolute measurements of Ehrhardt [25] in cases (a) and (b). Figure 2 displays five sets of results for the coplanar scattering corresponding to (a) $E_1=5$ eV, $\theta_2=4°$; (b) $E_1=5$ eV, $\theta_2=10°$; (c) $E_1=5$ eV,

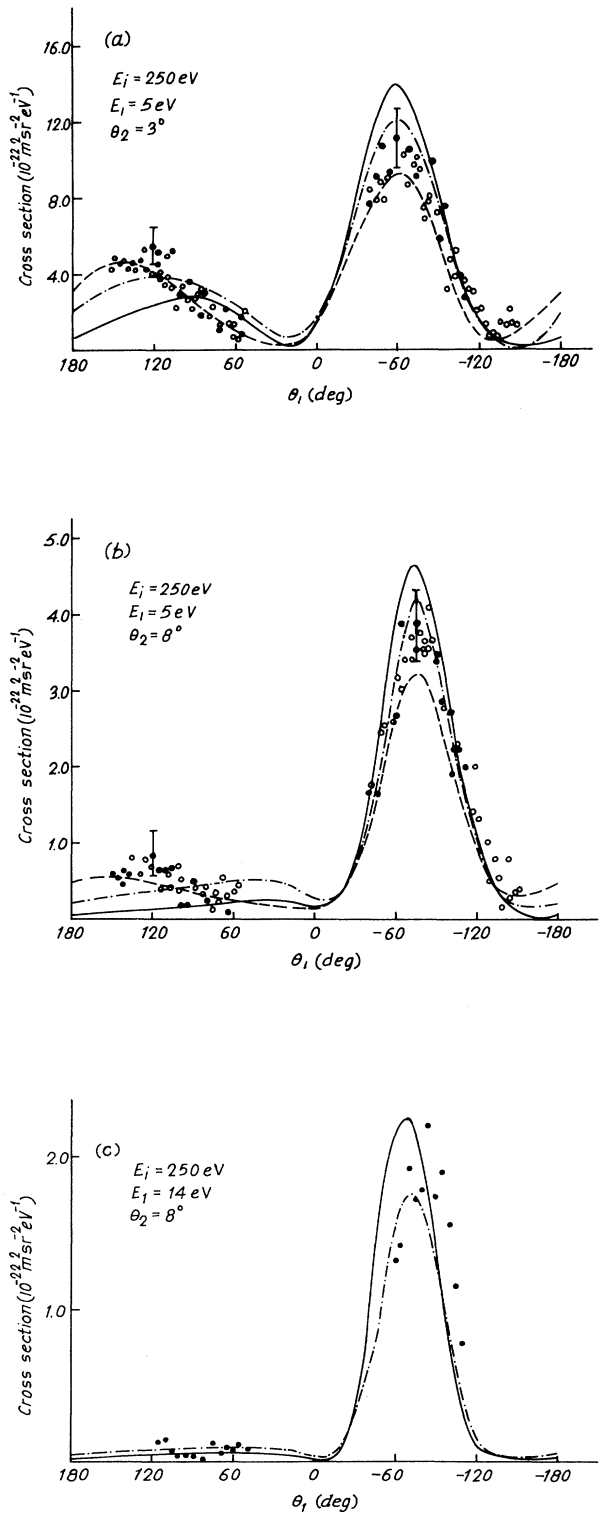

FIG. 1. TDCS for coplanar ionization of hydrogen atoms by electrons at $E_i = 250$ eV for (a) $E_1 = 5$ eV, $\theta_2 = 3°$; (b) $E_1 = 5$ eV, $\theta_2 = 8°$; and (c) $E_1 = 14$ eV, $\theta_2 = 8°$. Theory: ——, present calculation; — — —, Brauner, Briggs, and Klar [11]; —·—·—·, DWBA [16]. Experiment: ○, Ehrhardt *et al.*, [8,25]; ●, Lohmann *et al.* [24].

$\theta_2 = 16°$; (d) $E_1 = 3$ eV, $\theta_2 = 10°$; and (e) $E_1 = 10$ eV, $\theta_2 = 16°$. As in the previous case, the theoretical results we compare with are the DWBA results and the results of Brauner, Briggs, and Klar. Here, for the sake of comparison, we have the measured results of Ehrhardt only.

Now, considering all the small-momentum-transfer cross-section results together, it is clear that in the binary-peak region, the present results, the DWBA results, and the pseudostate calculation (the results of which are not shown here; see Ref. [16]) agree more or less with one another. In a few large-momentum-transfer cases [see Figs. 1(c) and 2(e)] the present results appear somewhat better, while in a few very-small-momentum-transfer cases [see Fig. 2(a)]; DWBA results appear to be little better. For positive θ_1, there are, however, considerable differences between the results of these various calculations. In this connection a few points may be noted. The first is that the overall shapes of the curves of the present calculation and of the DWBA calculation quite agree with each other but not with those of the experiments for positive values of θ_1. The second point to be noted is that for θ_1 ranging from 0° to about 75°, the present results agree quantitatively with the theoretical results of Brauner, Briggs, and Klar [11] and of the pseudostate calculation, and the general trend here is in agreement with the experimental results. DWBA results are too large in this region [see Fig. 2(d) in particular]. Beyond this, however, the present results, the DWBA results and the pseudostate results are all small compared to the experimental results, the present results being the smallest among these. Another point to be noted [see Figs. 2(a)–2(c)] is that for a fixed energy of the ejected electron, the DWBA calculation tends to overestimate the binary peak, but the present calculation tends to exactly estimate the binary peak as the scattering angle θ_2 increases. For a further check of the results, we evaluated the total cross section. Our results are less than the experimental results of Shah, Elliott, and Gilbody [26] by 5% and 20% at 250 and 150 eV, respectively. At these energies the DWBA results are greater than the experimental results by about the same percentages. Clearly, the reason for the smallness of our total cross-section result is the smallness of our TDCS results in the recoil region. At higher energies our calculation is in excellent agreement with the results of experiments regarding the total cross section.

It may also be noted here that the cross-section results obtained by using the unnormalized wave function (4b) are about three or four times larger than the correct results. The normalization factor N not only brings down the cross-section values to the desired level but nearly to the exact experimental values in most cases.

Figure 3 displays the large-momentum-transfer cross-section results for 413.6 eV, a relatively higher energy in the intermediate range. The two outgoing electron energies are equal to 200 eV. The figure displays three sets of results in a three-dimensional form corresponding to scattering angle $\theta_2 = 30°$, 40°, and 50°, the ejection angle θ_1 belonging to the range 30°–80°. Here, $\varphi_1 - \varphi_2 = \pi$. The present results have been compared with the distorted-wave-impulse-approximation [13] (DWIA) re-

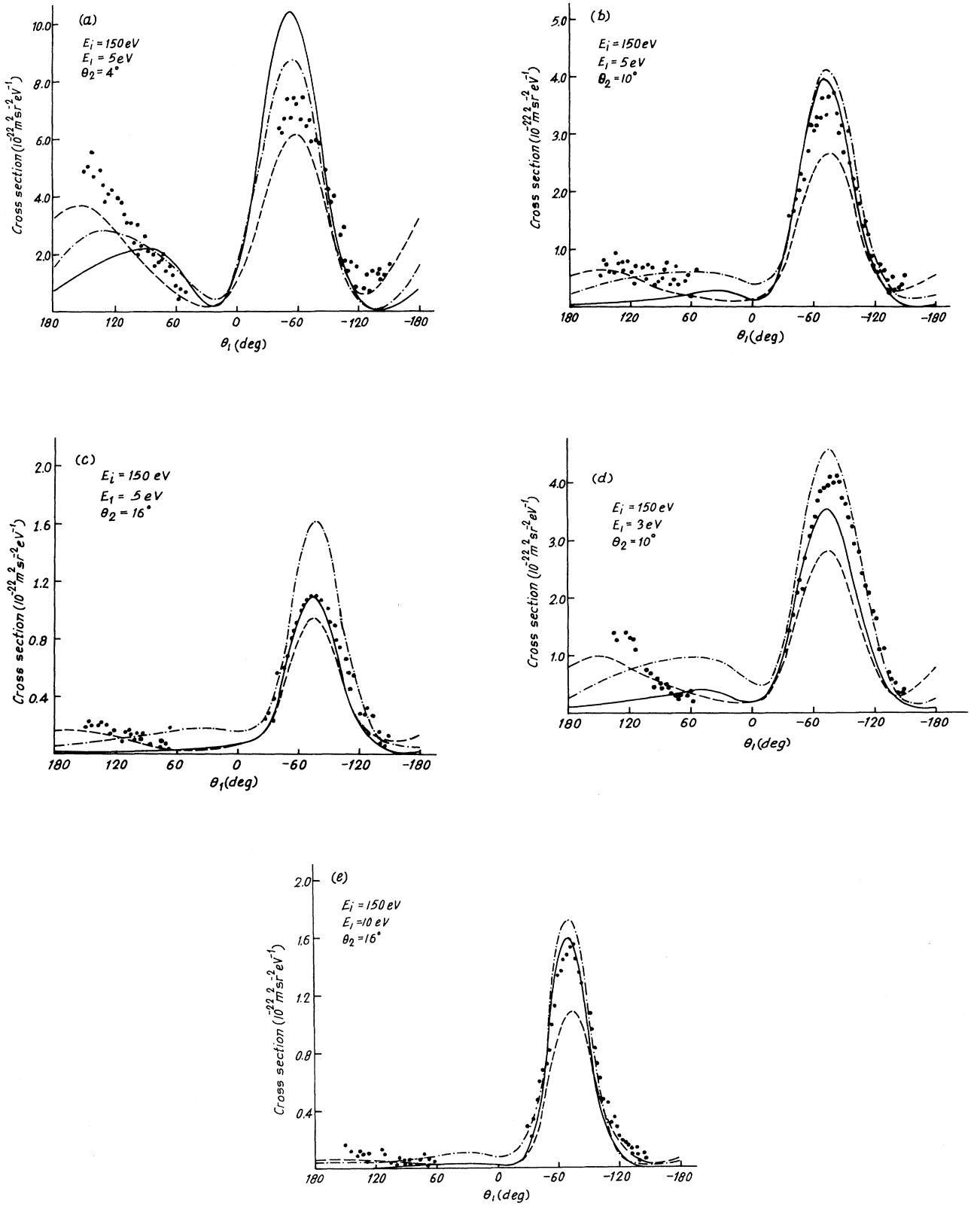

FIG. 2. TDCS for coplanar ionization of hydrogen atoms by electrons at $E_i = 150$ eV for (a) $E_1 = 5$ eV, $\theta_2 = 4°$; (b) $E_1 = 5$ eV, $\theta_2 = 10°$; (c) $E_1 = 5$ eV, $\theta_2 = 16°$; (d) $E_1 = 3$ eV, $\theta_2 = 10°$; and (e) $E_1 = 10$ eV, $\theta_2 = 16°$. Theory: ——, present calculation; — — —, Brauner, Briggs, and Klar [11]; —·—·—·, DWBA [16]. Experiment: ●, Ehrhardt *et al.* [8,25].

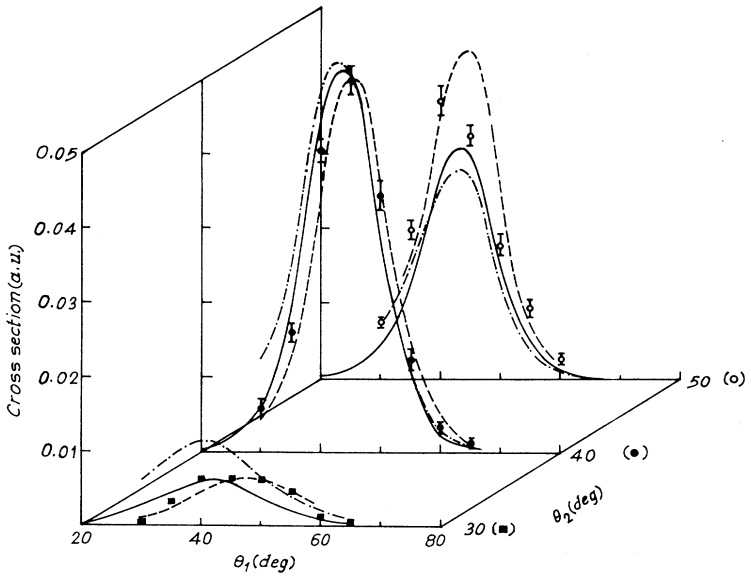

FIG. 3. TDCS for ionization of hydrogen atoms by electrons at $E_i=413.6$ eV, $E_i=E_1=200$ eV, θ_2 being fixed at 30°, 40°, and 50°, $\varphi_1-\varphi_2=\pi$, and θ_1 variable. Theory: ——, present calculation; — — —, DWIA [13] (X4.0); —·—·—·, PWBE (X1.5). Experiment: ■ (30°), ● (40°), ○ (50°), Weigold *et al.* [13] (normalized at $\theta_1=45°$, $\theta_2=40°$ with the present calculation).

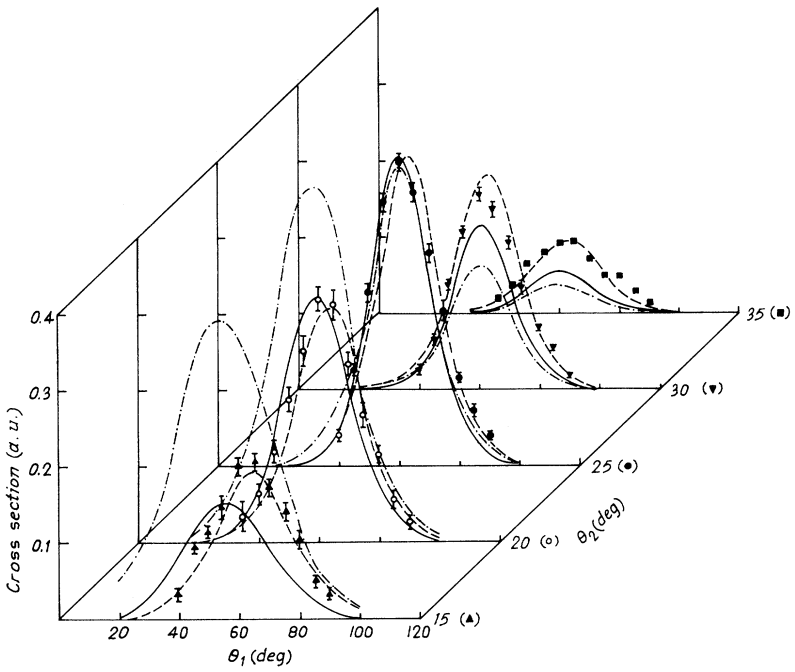

FIG. 4. TDCS for ionization of hydrogen atoms by electrons at $E_i=250$ eV, $E_1=50$ eV, θ_2 being fixed at 15°, 20°, 25°, 30°, and 35°, $\varphi_1-\varphi_2=\pi$ and θ_1 variable. Theory: ——, present calculation; — — —, DWIA [13] (X4.6); —·—·—·, PBWE (X1.1). Experiment: ▲ (15°), ○ (20°), ● (25°), ▼ (30°), ■ (35°), Weigold *et al.* [13] (normalized at $\theta_1=60°$, $\theta_2=20°$ with the present results).

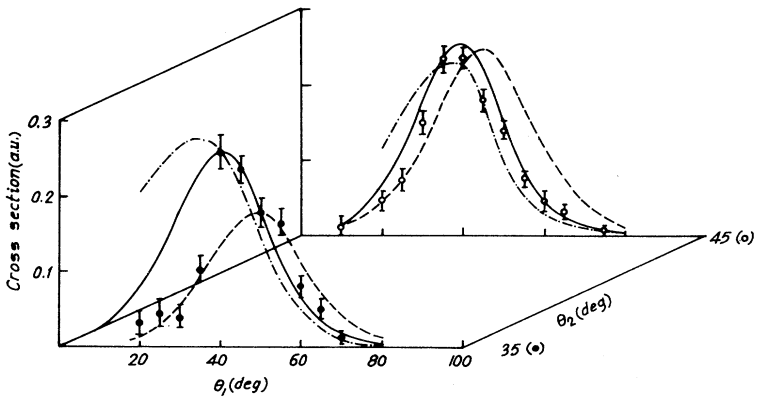

FIG. 5. TDCS for ionization of hydrogen atoms by electrons at $E_i=113.6$ eV, $E_1=E_2=50$ eV, θ_2 being fixed at 35° and 45°, $\varphi_1-\varphi_2=\pi$ and θ_1 variable. Theory: ——, present calculation; — — —, DWIA (X6.5); —·—·—·, PWBE (X0.83). Experiment: ● (35°), ○ (45°), Weigold *et al.* [13] (normalized at $\theta_1=40°$, $\theta_2=35°$ with the present result).

sults and with the plane-wave Born approximation with exchange (PWBE) [13] included. The results are also compared with the relative measured values of Weigold *et al.* [13]. Qualitative agreement between the present results and the measured results of Weigold *et al.* is very good, often better than those with PWBE results, but are similar to those with DWIA results. Quantitatively, however, the present results are about four times the DWIA results and are close to the PWBE results.

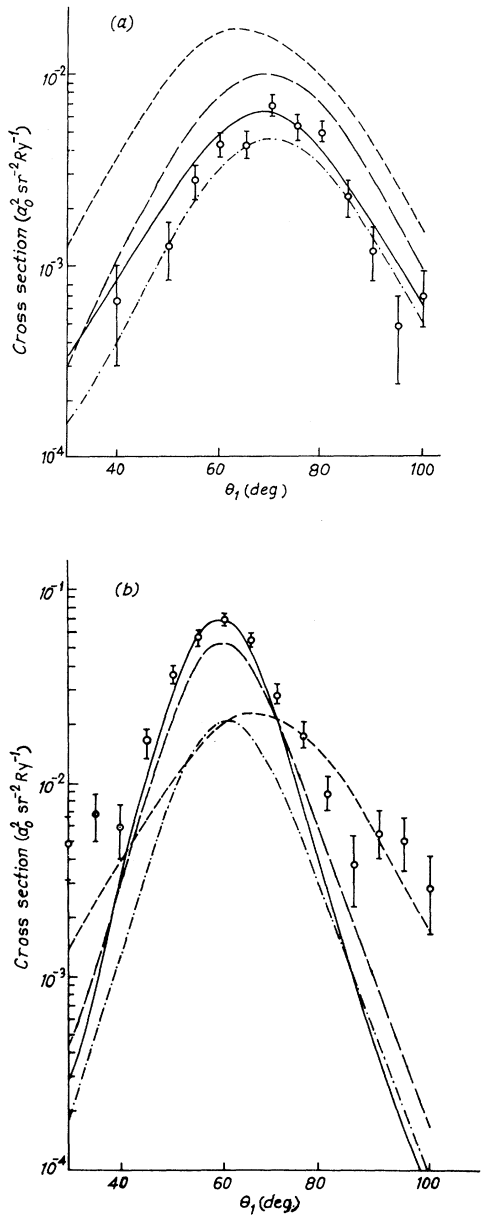

FIG. 6. TDCS for ionization of hydrogen atoms by electrons at $E_i=413.6$ eV for (a) $E_1=50$ eV, $\theta_2=30°$; (b) $E_1=100$ eV, $\theta_2=30°$, $\varphi_1-\varphi_2=\pi$ and θ_1 variable. Theory: ——, present calculation; — — —, DWBA [14]; —·—·—·, DWIA; — — —, B2. Experiment: ⊹, McCarthy *et al.* (normalized at a single point in each case).

Figure 4 displays the large-momentum-transfer cross-section results corresponding to 250-eV energy of the incident electron. The two outgoing electrons have energies of 50 and 186.4 eV, respectively. The figure displays five sets of results corresponding to $\theta_2=15°$, 20°, 25°, 30°, and 35° and θ_1 to the range 20°–100°, in a three-dimensional form. Here, $\varphi_1-\varphi_2=\pi$. Here, also, we compare our results with the relative experimental results of Weigold *et al.* [13] and with the theoretical results of DWIA [13] and PWBE [13] approximations. As before, qualitatively the present results are similar to the DWIA results and the experimental results. But numerically these are about four-and-a-half times the DWIA results and are closer to the PWBE results.

Figure 5 shows results for incident-electron energy of 113.6 eV, while the two outgoing electrons have equal energies of 50 eV. Here two sets of results are presented corresponding to $\theta_2=35°$ and 45° and $\varphi_1-\varphi_2=\pi$. These are compared with DWIA results [13], PWBE results [13] and with the relative measurements of Weigold *et al.* [13]. The results of the present calculations correctly reproduce the peaks, the peak positions as well as the relative peak heights. Here the results are much better compared to the DWIA results and the PWBE results. Numerically the present results are about six-and-half times the DWIA results and are closer to the PWBE results.

Figure 6 displays coplanar-scattering cross-section results for incident-electron energy of 413.6 eV, scattering angle $\theta_2=30°$, and for two different values of ejected electron energy (a) $E_1=50$ eV and (b) $E_1=100$ eV. The above scattering parameters correspond to relative measurement of McCarthy *et al.* [14]. Here we compare our results with the above measured values of McCarthy *et al.* and with the theoretical results of second Born approximation, DWBA [14], and DWIA [14] approximations. Except for $B2$ cross-section curves, the other theoretical cross-section curves are very similar in shape. The $B2$ cross-section results grossly disagree with the experimental values. Our results are closer to the DWBA results and are considerably larger than the DWIA results. Rembering that the energy 413.6 eV is a relatively high energy, the above closeness between our results and the results of DWBA goes in favor of the above calculations and goes against the DWIA calculation. However, still, there are large differences between the DWBA and the present results, and some absolute measured results are necessary for further discrimination.

IV. CONCLUSIONS

The present calculation, which uses the three-particle continuum wave function of Das [21] and incidentally which is the same as the first-order Faddeev wave function, after a proper normalization, describes satisfactorily the measured cross-section results of Ehrhardt [25] for small-momentum-transfer cases except for a (certain) region which includes the experimental recoil peak and which becomes unimportant with the increase of the momentum transfer. The calculation also describes the large-momentum-transfer cross-section results qualita-

tively. The agreement of the present results with the coupled pseudostate calculation and with the DWBA calculation is quite remarkable. In fact the total cross sections calculated by the present method and by the DWBA method are of the same order of accuracy. For 250 eV, for example, the present calculation gives a value which is only 5% less than that of experiment, while the DWBA result is 5% greater than the experimental value. Now for larger-momentum transfer cases there are large differences in quantitative results of these two calculations [see Figs. 1(c) and Fig. 6] but qualitatively these are very similar. Since the present calculation is expected to be more accurate for larger-momentum-transfer cases, its results may be favored by experiments. The present calculation takes the electron-electron correlation in the final channel symmetrically and exactly to the first order. There is scope for inclusion of higher-order effects in the calculation. So the present calculation may be considered as the first step in a systematic improvement of an ionization calculation. The present calculation is also simple. Here, the scattering amplitude contains several terms. Each involves integration with one Coulomb wave only, the result ultimately depending at most on a single integration over [0,1] of a smooth function. The form of the scattering amplitude may help in an analysis of the scattering mechanism for any particular kinematic condition. For example, the dominance of a particular term will indicate which physical effect is the most important there. Single- and double-differential cross sections are also easily obtainable from it. The calculation may be generalized for application to the ionization of other atoms and ions.

ACKNOWLEDGMENTS

One of the authors (S.S.) is grateful to the CSIR for support. They are also thankful to the Director, VEC Centre, Calcutta, for giving permission to use their ND500 computer system for the necessary computational work.

[1] C. A. Quarles and J. D. Faulk, Phys. Rev. Lett. **31**, 859 (1973).
[2] J. N. Das, Nuovo Cimento B **12**, 197 (1972).
[3] J. N. Das and S. Chakraborty, Phys. Rev. A **32**, 176 (1985); Phys. Lett. A **92**, 127 (1982).
[4] D. H. Madison and E. Merzbacher, *Atomic Inner-Shell Processes,* edited by B. Crasemann (Academic, New York, 1975), Vol. I, p. 1.
[5] M. Komma and W. Nakel, J. Phys. B **12**, 1587 (1979); **15**, 1433 (1982).
[6] H. Ruoff and W. Nakel, J. Phys. B **20**, 2299 (1987).
[7] A. Stahl, J. Bonfert, H. Graf, and W. Nakel, J. Phys. B **22**, 3747 (1989).
[8] H. Ehrhardt, K. Jung, G. Knoth, and P. Schlemmer, Z. Phys. D **1**, 3 (1986).
[9] E. P. Curran and H. R. J. Walters, J. Phys. B **20**, 337 (1987); **20**, 1105 (1987).
[10] S. Sharma and M. K. Srivastava, Phys. Rev. A **35**, 1939 (1987).
[11] M. Brauner, J. S. Briggs, and H. Klar, J. Phys. B **22**, 2265 (1989).
[12] I. E. McCarthy and E. Weigold, Phys. Rep. C **27**, 275 (1976).
[13] E. Weigold, C. J. Noble, S. T. Hood, and I. Fuss, J. Phys. B **12**, 291 (1979).
[14] I. E. McCarthy, E. Weigold, X. Zhang, and Y. Zheng, J. Phys. B **22**, 931 (1989).
[15] R. Müller-Fielder, P. Schlemmer, J. Jung, and H. Ehrhardt, Z. Phys. A **320**, 89 (1985).
[16] I. E. McCarthy and X. Zhang, Aust. J. Phys. **43**, 291 (1990); for an earlier formulation of DWBA, see D. H. Madison, R. V. Calhoun, and W. N. Shelton, Phys. Rev. A **16**, 552 (1977); B. H. Bransden, J. J. Smith, and K. H. Winters, J. Phys. B **11**, 3095 (1978).
[17] S. M. Younger, Phys. Rev. A **24**, 1272 (1981).
[18] I. E. McCarthy and X. Zhang, J. Phys. B **22**, 2189 (1989).
[19] J. N. Das and Samita Seal, Z. Phys. D **21**, 23 (1991).
[20] J. N. Das and P. K. Bhattacharyya, J. Phys. B **23**, L145 (1990); **25**, 249 (1992).
[21] J. N. Das, Phys. Rev. A **42**, 1376 (1990).
[22] L. D. Faddeev, Zh. Eksp. Teor. Fiz. **39**, 1459 (1960) [Sov. Phys. JETP **12**, 1014 (1961)].
[23] R. R. Lewis, Phys. Rev. **102**, 537 (1956).
[24] B. Lohmann, I. E. McCarthy, A. T. Stelbovics, and E. Weigold, Phys. Rev. A **30**, 758 (1984).
[25] H. Ehrhardt (private communication).
[26] M. B. Shah, D. S. Elliot, and H. B. Gilbody, J. Phys. B **20**, 3501 (1987).